



Longwave radiation at the earth's surface in Estonia

Viivi Russak^{a*} and Ingrid Niklus^b

^a Tartu Observatory, 61602 Tõravere, Tartumaa, Estonia

^b Estonian Environment Agency, Mustamäe tee 33, 10616 Tallinn, Estonia

Received 24 January 2015, revised 20 March 2015, accepted 25 March 2015, available online 26 November 2015

Abstract. Solar radiation has been continuously measured in Estonia since 1950, but the recordings of longwave radiation began only about ten years ago. This paper presents the first description of the characteristic features of up- and downwelling longwave radiation in the Baltic Sea region. In the radiation balance the longwave fluxes have an important role. In the annual totals of radiation incident upon the ground surface in Estonia, the longwave atmospheric downwelling radiation $L_{1\downarrow}$ exceeds the direct solar radiation $E_{g\downarrow}$ about three times, and this ratio has an essential seasonal run. In the total upwelling radiation $L_{1\uparrow}$, the infrared part is still greater, up to 92%. Comparing the measured and calculated (according to the Stefan–Boltzmann law) hourly totals of $L_{1\uparrow}$ for snow (emissivity $\varepsilon = 0.85$) we found a good linear relationship ($R^2 = 0.96$). However, the measured totals systematically exceeded the calculated values (on average by 18%). Dependence of the downwelling infrared radiation $L_{1\downarrow}$ on the near-surface water vapour pressure e is approximated by a power function ($R^2 = 0.73$). This is in good accordance with the results of studies carried out at other geographical sites. The influence of clouds on the fitted power function is noteworthy. Separate analysis of the hours with full cloudiness of low clouds and the cloudless hours confirmed the validity of the power function. However, a difference was found in their parameters (for overcast sky the exponent $b = 0.20$, $R^2 = 0.91$ and for cloudless sky $b = 0.25$ and $R^2 = 0.93$).

Key words: longwave radiation, upwelling radiation, downwelling radiation, water vapour pressure, cloudiness, annual course, diurnal course, frequency.

1. INTRODUCTION

The net radiation at the earth's surface is of dominant importance in studies of climate changes. Often the short- and longwave contributions to the radiation budget have been studied separately. Solar radiation has been continuously measured in many geographical sites during long periods. However, similar studies of longwave radiation started mostly after the Baseline Surface Radiation Network (BSRN) was established as a project of the World Climate Research Programme (WCRP) in 1992. In Estonia continuous solar radiation measurements began in 1950. The characteristic features of shortwave components of net radiation in Estonia, found based on long time series, are described in the handbook by Russak and Kallis (2003). Systematic recordings of longwave radiation were started here only about ten years ago, and due to the shortness of these time series,

no results of corresponding analysis have been published hitherto.

During the last decades, interest in the role of longwave radiation has increased considerably. This can be due to the role of atmospheric longwave radiation in enhancing the greenhouse effect, resulting in global warming. As thermal radiation depends on several meteorological parameters, e.g. on temperature and humidity and their profiles, cloudiness, atmospheric aerosol content, etc., infrared radiation varies both seasonally and geographically. At present, the amount of collected data on longwave radiation at several sites is sufficient to highlight its characteristic features.

2. DATA

In the present study the hourly totals (MJ m^{-2}) of up- and downwelling longwave radiation recorded at Tartu-Tõravere meteorological station of the Estonian Environ-

* Corresponding author, viivi.russak@to.ee

ment Agency (58°16'N, 26°28'E, $h = 70$ m a.s.l.) are used to study the features of the longwave components of the near-surface radiation budget in Estonia. Silicon-domed Eppley PIR pyrgeometers, installed at 2 m above a grassy surface, were used as receivers of longwave radiation. The instrument for recording downwelling atmospheric radiation L_{\downarrow} was shaded from direct solar rays by a tracking shading disc. Initially the receivers were calibrated in the World Radiation Centre in Davos, Switzerland. Continuous recording of downwelling atmospheric radiation L_{\downarrow} began in 2003, that of upwelling fluxes (L_{\uparrow}) in July 2006. The meteorological data necessary for analysis, i.e. the hourly mean bare soil temperature t (°C) and water vapour pressure e (hPa), were obtained using a Vaisala automatic weather station AMS520. The genera and amount of high, middle, and low clouds were visually determined in tenths at 1-hour intervals during daylight hours and at 3-hour intervals at night. Tartu-Tõravere station is located in a rural area with no outdoor lighting. In our case, we used extreme conditions (cloudless and 10 tenths of low clouds), which are at night reliably determined by the visibility of stars. At Tõravere an observer-staffed station operates with 24-hour maintenance of instruments.

3. UPWELLING LONGWAVE RADIATION

The upwelling longwave radiation L_{\uparrow} depends mainly on surface temperature and slightly on surface properties. In the range of surface temperatures t observed at Tõravere in 2007–2012 (from -27 to $+32$ °C) the 2045 hourly totals of upwelling longwave radiation were credibly described by a linear relationship (Eq. 1), (Fig. 1):

$$L_{\uparrow} = 0.017 t + 1.146, R^2 = 0.98. \quad (1)$$

The significance level $p < 0.01$.

According to the Stefan–Boltzmann law, the upwelling longwave radiation is proportional to the fourth power of the absolute temperature T^4 of ground surface. The linear dependence in our results is due to the circumstance that the Stefan–Boltzmann law holds for a full range of temperatures, but for narrow temperature ranges it reduces well to a linear dependence. To compare the consistence of measured and calculated L_{\uparrow} hourly totals separately, we analysed the observational data recorded at hours with snow cover (depth of snow

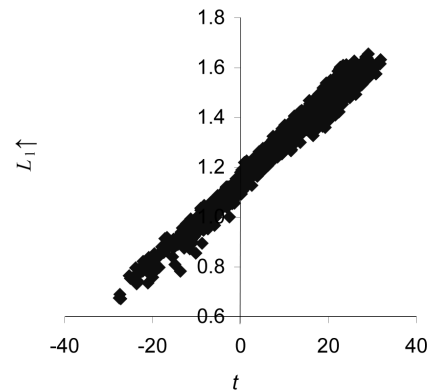


Fig. 1. Dependence of the hourly totals of upwelling longwave radiation L_{\uparrow} (MJ m⁻²) on ground surface temperature t (°C) in Estonia, 2007–2012.

at least 3 cm). The radiation emissivity ϵ of snow depends on its structure and varies from 0.8 to 0.9 (e.g. www.monarchserver.com, www.omega.com). Our calculations for 534 hourly totals were carried out with the Stefan–Boltzmann formula, adopting $\epsilon = 0.85$. We plotted the measured L_{\uparrow} values against those calculated by the Stefan–Boltzmann law and found a good linear relationship ($R^2 = 0.96$). However, the measured totals of L_{\uparrow} systematically exceeded the calculated values (on average by 18%).

In case of grassy surface, this kind of comparison was impossible. Problems emerged how to estimate the temperatures. The ground temperatures were measured on bare soil and, as known, the soil temperatures are typically higher than those of grass. Unfortunately, no reasonable relation between soil and grass temperatures was available to us.

In Estonia the annual totals of the longwave radiation emitted by the ground surface constituted on average 11 071 MJ m⁻² during the period 2007–2012. The proportions of different monthly totals in the annual sum vary on average from 6% (in February) to 10% (in July) (Table 1).

The inter-annual fluctuations of the L_{\uparrow} monthly totals are small: in winter the coefficient of variation $V = 6$ –9%, in summer 1–3%. The hourly totals pose a greater challenge (Fig. 2). The corresponding values of the coefficient of variation $V = 12$ –14% in winter and 9–11% in summer. The greatest hourly total of L_{\uparrow} , 1.923 MJ m⁻², was recorded on 8 July 2011, the smallest, 0.609 MJ m⁻², on 5 February 2012.

Table 1. Mean monthly totals of upwelling longwave radiation L_{\uparrow} and their standard deviations (MJ m⁻²) at Tõravere, 2007–2012

	Jan	Feb	March	Apr	May	June	July	Aug	Sep	Oct	Nov	Dec
Totals	786.3	688.9	837.1	902.2	1022.5	1043.6	1123.6	1085.6	975.2	938.2	851.9	816.5
SD	53.8	64.9	33.8	12.8	12.0	24.8	34.0	26.9	12.8	27.9	19.9	47.8

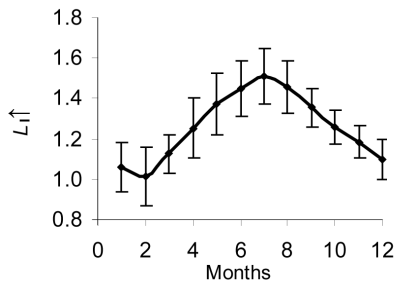


Fig. 2. Averaged hourly totals of upwelling longwave radiation $L_1\uparrow$ in different months and their standard deviations (MJ m^{-2}) in Estonia, in 2007–2012.

The diurnal course of the $L_1\uparrow$ hourly totals is rather marginal in winter months. The difference between their values in day- and night-time hours is evident only in the warm season, when incident solar radiation heats the ground. The difference between noon and midnight surface temperatures is practically lacking in winter, but in summer its diurnal amplitude is up to 15°C on average. The greatest average difference (about 20%) between the hourly sums of $L_1\uparrow$ at noon and at midnight was observed in April (Fig. 3). This is evidently due to the diurnal course of ground temperature. In Estonia April is the main transitional time from cold to warm season conditions, when the ground is usually covered with old grass or snow, or both.

The shape of the frequency distribution over the set of the recorded hourly totals is asymmetrical. While all the values varied within the range from 0.61 to 1.92 MJ m^{-2} , about half of them were in the interval $1.13\text{--}1.37 \text{ MJ m}^{-2}$ (Fig. 4).

The distribution varies during the year, being almost symmetric in summer, but strongly skewed towards smaller values in the winter months. In winter a weak secondary maximum is noticeable, corresponding to frosty days (Fig. 5).

Besides longwave radiation, the earth’s surface also loses radiation energy as reflected solar radiation $E_r\uparrow$.

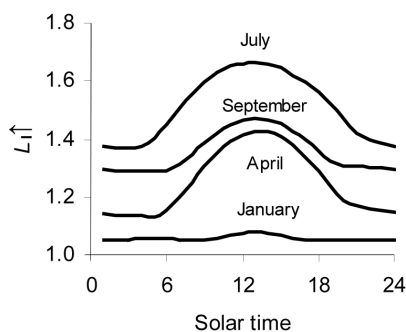


Fig. 3. Mean diurnal courses of the hourly totals of upwelling longwave radiation $L_1\uparrow$ (MJ m^{-2}) in Estonia in January, April, July, and September 2007–2012.

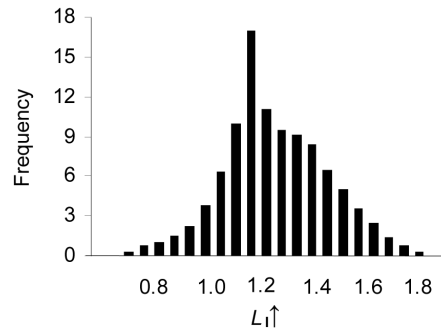


Fig. 4. Frequency distribution (%) of the hourly totals of upwelling longwave radiation $L_1\uparrow$ (MJ m^{-2}) recorded in Estonia during 2007–2012.

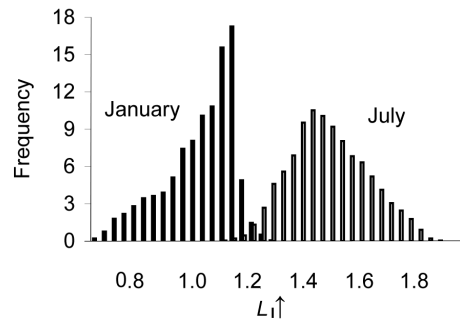


Fig. 5. Frequency distribution (%) of the hourly totals of upwelling longwave radiation $L_1\uparrow$ (MJ m^{-2}) in Estonia in January and July, 2007–2012.

However, the role of the latter in the completely upwelling radiation is small. About 92% of the annual totals of the leaving radiation is due to $L_1\uparrow$. Only in March, when the combined impact of increased solar radiation and high albedo of snow abruptly increases the reflected solar radiation, does the role of $L_1\uparrow$ fall to 85% (Fig. 6).

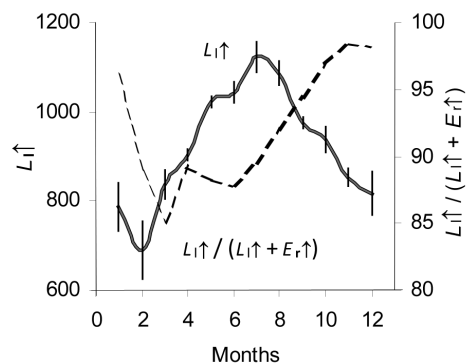


Fig. 6. Annual course of the averaged monthly sums of upwelling longwave $L_1\uparrow$ with the corresponding standard deviations (MJ m^{-2}) and the role of $L_1\uparrow$ in pan-spectral upwelling radiation $L_1\uparrow/(L_1\uparrow + E_r\uparrow)$, %.

4. DOWNWELLING LONGWAVE RADIATION

In comparison with upwelling longwave radiation, the downwelling atmospheric radiation L_{\downarrow} is more variable due to its dependence on several factors (e.g. L_{\uparrow} ; air temperature; the content of water vapour, CO_2 , O_3 , CH_4 , N_2O , CF, as well as some kinds of aerosols and also their vertical profiles). The annual total of L_{\downarrow} averaged over the period 2003–2012 added up to 9808 MJ m^{-2} at Tõravere. Its inter-annual variability is small (the coefficient of variation $V=0.01$) and the proportion of different monthly totals in annual totals rises from 6–7% in winter to 9–10% in summer (Table 2).

The diurnal course of the hourly totals of the atmospheric longwave radiation is small: over a 24-hour period, hourly totals change relatively just a bit. The difference between the totals in daytime and at night is practically lacking in winter. Even in summer, the totals of L_{\downarrow} at noon exceed their values at midnight only by about 8% (Fig. 7). Its greatest hourly total, 1.584 MJ m^{-2} , was recorded on 15 July 2010, the smallest, 0.472 MJ m^{-2} , on 19 January 2006.

The frequency distribution of the hourly totals of L_{\downarrow} is monomodal and negatively skewed (Fig. 8). Over the course of a year, the shape of the distribution varies basically as follows: in summer it is monomodal and in January–February bimodal, where the mode at smaller values corresponds to the cloudless frosty hours (Fig. 9).

The contribution of L_{\downarrow} to the downward component of the radiation balance is greater than that of solar

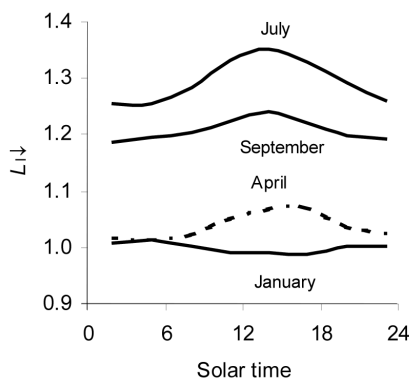


Fig. 7. Mean diurnal course of the hourly totals of downwelling longwave radiation L_{\downarrow} (MJ m^{-2}) in Estonia in January, April, July, and September 2003–2012.

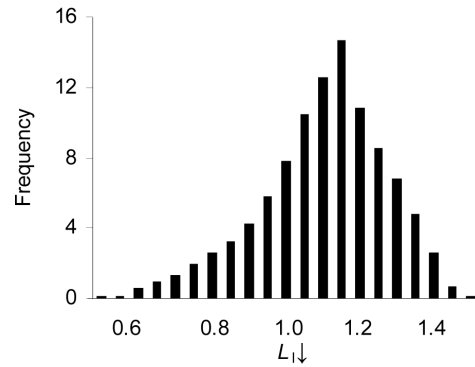


Fig. 8. Frequency distribution (%) of the hourly totals of downwelling longwave radiation L_{\downarrow} (MJ m^{-2}) in Estonia, 2003–2012.

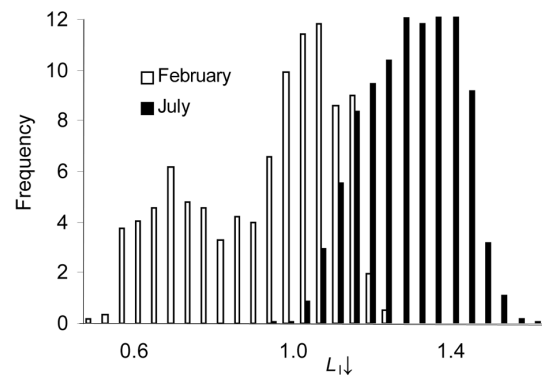


Fig. 9. Frequency distribution (%) of the hourly totals of downwelling longwave radiation L_{\downarrow} (MJ m^{-2}) in Estonia in February and July 2003–2012.

radiation (Fig. 10). Annual totals of L_{\downarrow} exceed those of global radiation $E_{\text{g}\downarrow}$ about three times. Over the course of a year this ratio, that is $L_{\downarrow}/E_{\text{g}\downarrow}$, varies largely.

In winter longwave radiation is crucial in the incoming radiation: from November to January its role is as high as 95–97%. From May to July the contributions of L_{\downarrow} and $E_{\text{g}\downarrow}$ become closer, and then the totals of atmospheric radiation comprise about 60% of the entire downwelling radiation. This type of great annual variability is mainly caused by the annual cycle of solar radiation. The latter in turn is highly dependent on the annual course of solar elevation and the duration of light time. In Estonia the solar elevation reaches about 55°

Table 2. Mean monthly totals of downwelling longwave radiation L_{\downarrow} and their standard deviations (MJ m^{-2}) at Tõravere, 2003–2012

	Jan	Feb	March	Apr	May	June	July	Aug	Sep	Oct	Nov	Dec
Totals	740.4	638.5	732.1	747.2	847.4	873.7	963.1	955.1	870.5	853.6	802.7	780.7
SD	40.5	54.6	49.1	17.3	25.8	14.8	32.3	19.4	14.3	32.5	24.7	35.8

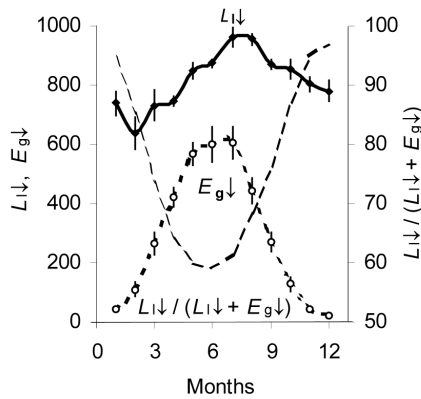


Fig. 10. Mean annual courses of monthly totals of incident upon ground surface solar global radiation $E_{g\downarrow}$ and downwelling longwave radiation $L_{1\downarrow}$ with their standard deviations (MJ m^{-2}) and the role of $L_{1\downarrow}$ in the total all-wave incoming radiation (%) in Estonia, 2003–2012.

and light time duration is 18 hours at noon on the summer solstice, on the winter solstice the corresponding values are only about 8° and 6 hours. In addition, the annual courses of the amount and genera of clouds play an important role (Fig. 11, Table 3). The optically thick low clouds, which intensively attenuate solar radiation simultaneously increasing atmospheric radiation, have the opposite impact on short- and longwave radiation.

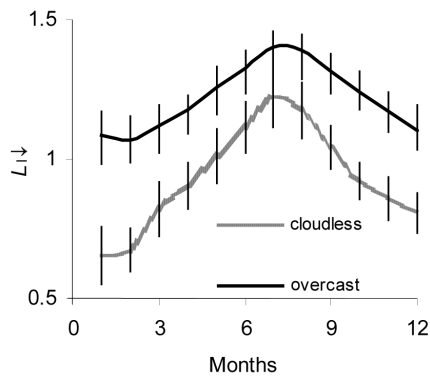


Fig. 11. Mean annual course of hourly totals of downwelling longwave radiation $L_{1\downarrow}$ and the corresponding standard deviations (MJ m^{-2}) in cloudless skies and overcast by low clouds skies in Estonia, 2003–2012.

5. FACTORS AFFECTING DOWNWELLING LONGWAVE RADIATION

Among the numerous factors affecting the fluxes of downwelling atmospheric radiation, water vapour is the dominant one. Although its emissivity is lower than, for example, that of CO_2 or CH_4 , water vapour plays an essential role in the generation of counter-radiation fluxes owing to its higher abundance in the atmosphere. Due to the temporal and spatial variability of the atmospheric water content, the incoming longwave radiation can differ geographically. The atmospheric radiation depends not only on the amount of water vapour, but also on its vertical profile and temperature. No suitable data on the corresponding gradients were at our disposal. Therefore we decided to use here the relationship between near-surface water vapour pressure e (hPa) and hourly totals of downwelling longwave radiation $L_{1\downarrow}$ (MJ m^{-2}). The choice was made taking into account that the near-ground humidity parameters depend linearly on the total amount of water vapour in the vertical air column (e.g. Okulov, 2003; Ruckstuhl et al., 2007; Kannel et al., 2012) and the lowermost air layers are dominant for the vertical gradient of water vapour.

From analysis of the corresponding data for 20 355 hours from the period 2006–2012 it followed that the dependence between e and $L_{1\downarrow}$ was best described by a power function (Eq. 2), (Fig. 12):

$$L_{1\downarrow} = 0.704 e^{0.23}, \text{ where } R^2 = 0.73. \quad (2)$$

Our result fits well the relationships between specific humidity and incoming longwave radiation obtained from the analysis of measurement data from BSRN as well as some other actinometrical stations (Ruckstuhl et al., 2007; Stanhill, 2011; Rosa and Stanhill, 2014). A slightly different result from our Eq. (2) was obtained for Tõravere observations by Rosa and Stanhill (2014) (exponent $b = 0.22$). It is interesting to note that we found a good accordance between the results by Stanhill (2011) for Valentia (Ireland) and our results for Tõravere. It is likely that this can partially be explained by similar air humidity and cloudiness conditions at these sites.

Table 3. Mean hourly totals of downwelling longwave radiation $L_{1\downarrow}$ and the corresponding standard deviations (MJ m^{-2}) in cloudless conditions ($y = 0$) and in overcast by low clouds ($m = 10$) conditions in Estonia, 2003–2012

	Jan	Feb	March	Apr	May	June	July	Aug	Sep	Oct	Nov	Dec
$L_{1\downarrow} (y = 0)$	0.655	0.675	0.823	0.907	1.012	1.113	1.225	1.176	1.042	0.924	0.860	0.808
SD	0.102	0.077	0.097	0.083	0.097	0.092	0.110	0.100	0.078	0.065	0.078	0.074
$L_{1\downarrow} (m = 10)$	1.087	1.068	1.122	1.176	1.258	1.328	1.404	1.390	1.314	1.242	1.173	1.106
SD	0.083	0.087	0.075	0.056	0.075	0.061	0.054	0.061	0.066	0.072	0.069	0.088

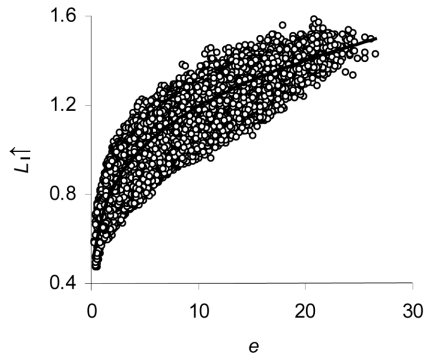


Fig. 12. Dependence of the hourly totals of downwelling longwave radiation $L_{1\downarrow}$ (MJ m^{-2}) on near-surface water vapour pressure e (hPa) at Tõravere, 2006–2012.

In Estonia the power relationship between e and $L_{1\downarrow}$ is stronger in winter than in summer ($R^2 = 0.76\text{--}0.78$ in January–February and $R^2 = 0.41\text{--}0.42$ in June–July). This is most likely caused by the differences in the mean vertical profiles of water vapour and temperature in cold and warm seasons. In the latter case, intensive air convection and turbulence carry humidity from the near-surface layers upwards, thus decreasing the relative role of the lowermost layers in the process of $L_{1\downarrow}$ formation. In addition, the variations in cloudiness conditions in the course of a year affect this dependence.

In order to estimate the contribution of clouds to the fitted power function, we analysed the data of the hours with 10 tenths of low clouds (7950 hours) separately from those of the hours for clear sky (2328 hours). In both cases the power relationship holds, but a difference was found in their parameters (Fig. 13). The corresponding approximations are

$$L_{1\downarrow} = 0.796 e^{0.20}, R^2 = 0.93, \text{ overcast with low clouds;} \quad (3)$$

$$L_{1\downarrow} = 0.601 e^{0.25}, R^2 = 0.91, \text{ clear sky.} \quad (4)$$

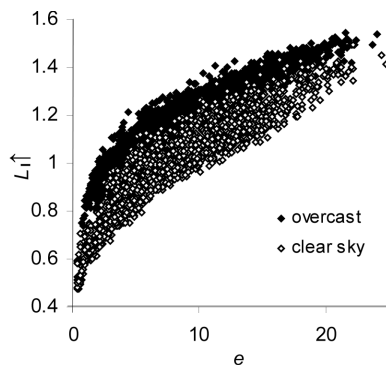


Fig. 13. Dependence of hourly totals of downwelling longwave radiation $L_{1\downarrow}$ (MJ m^{-2}) on near-surface water vapour pressure e (hPa) in the clear-sky and overcast with low clouds conditions.

Table 4. Parameters of the power relationship between hourly totals of downwelling longwave radiation $L_{1\downarrow}$ (MJ m^{-2}) and hourly mean water vapour pressure e (hPa) in different months in cloudless and overcast with low clouds conditions at Tõravere, 2006–2012

	Covered by 10 tenths of low clouds				Cloudless			
	a	b	R^2	Hours	a	b	R^2	Hours
Jan	0.798	0.20	0.87	1121	0.601	0.20	0.89	150
Feb	0.807	0.19	0.90	822	0.625	0.17	0.71	229
March	0.763	0.23	0.82	705	0.583	0.26	0.80	249
Apr	0.814	0.19	0.71	431	0.651	0.21	0.51	308
May	0.814	0.19	0.74	269	0.684	0.20	0.51	303
June	0.792	0.20	0.73	336	0.580	0.27	0.52	231
July	0.756	0.22	0.62	191	0.546	0.30	0.62	211
Aug	0.728	0.23	0.70	353	0.544	0.30	0.64	203
Sep	0.769	0.21	0.70	497	0.550	0.28	0.80	192
Oct	0.785	0.21	0.80	844	0.569	0.26	0.75	116
Nov	0.778	0.21	0.81	1148	0.572	0.25	0.71	66
Dec	0.800	0.20	0.88	1234	0.641	0.17	0.84	76

Within the limits of water vapour pressure in Estonia (0.5–25 hPa), 10 tenths of low clouds enlarge the counter-radiation on average by 12–37%. This effect is greater at smaller values of e , which are characteristic for the winter months. During cloudless hours about 91% of the variations in atmospheric downward radiation in Estonia can be attributed to the variations in the near-ground water vapour pressure. It is remarkable that also this effect is greater in winter months. In summer R^2 remains in the range of 0.5–0.6 (Table 4).

6. CONCLUSIONS

The aim of the present study is to describe the features of longwave radiation in Estonia and their dependence on the ground temperature, water vapour pressure, and cloudiness. Here we present the main conclusions.

In the annual totals of the incoming radiation, the atmospheric downwelling longwave radiation exceeds solar radiation about three times. This ratio has an essential seasonal course, which depends mainly on the annual solar cycle (solar elevation and the duration of light time) and on cloudiness conditions. In the annual totals of upwelling radiation, the proportion of longwave radiation is even greater than it is for downwelling radiation, constituting on average 92%. In comparison with solar radiation, the totals of longwave radiation are more stable.

In the limited range of ground temperatures t in Estonia during 2007–2012 (from -27 to $+32$ °C) the dependence of $L_{1\uparrow}$ on t is linear ($R^2 = 0.98$). Comparison of the measured $L_{1\uparrow}$ values and those calculated by the Stefan–Boltzmann law for snow (emissivity $\varepsilon = 0.85$)

showed a good linear relationship ($R^2 = 0.96$). However, the measured totals of $L_1\uparrow$ were systematically higher (on average by 18%).

The downwelling atmospheric radiation $L_1\downarrow$ depends mainly on the atmospheric water vapour distribution. Between the hourly totals of the atmospheric radiation and near-surface water vapour pressure e , a power function fitted. The parameters of the relationship vary considerably, depending on the cloudiness conditions. Within the limits of e observed in Estonia (0.5–25 hPa), 10 tenths of low clouds increase the downwelling atmospheric radiation on average by 12–37%. This effect is greater at smaller values of humidity, typical in Estonia during the winter months. In cloudless hours, about 91% of the variation in atmospheric radiation is connected to the variations in the near-ground water vapour pressure. It is characteristic that the dependence of $L_1\downarrow$ on e is stronger in winter months. This is most likely caused by differences in the mean vertical profiles of moisture and temperature in cold and warm seasons.

As our radiation time series is short, we could not find any statistically significant trends either for $L_1\uparrow$ or for $L_1\downarrow$. Our results, obtained based on this short time series and considering the small temporal variability of longwave radiation, fix the current main characteristic features of longwave radiation in local conditions. Tartu-Tõravere meteorological station is one of the few places in North Europe where components of the longwave radiation balance have been measured. As the weather in the Baltic Sea region is determined mainly by the cyclones moving eastwards from the Atlantic Ocean, the conditions of temperature, humidity, cloudiness, and other meteorological parameters that determine longwave radiation are quite similar all over Estonia. We even surmise that the description of near-surface longwave radiation presented in this paper can

approximately be characteristic not only for Estonia, but also for the whole territory around the Baltic Sea.

ACKNOWLEDGEMENTS

We are grateful to the European Regional Development Fund for supporting the investigation within the project 'Estonian Radiation Climate'. We thank the Estonian Environment Agency for making available the radiation and meteorological database of Tartu-Tõravere meteorological station.

REFERENCES

- Kannel, M., Ohvril, H., and Okulov, O. 2012. A shortcut from broadband to spectral aerosol optical depth. *Proc. Estonian Acad. Sci.*, **61**, 266–278.
- Okulov, O. 2003. *Variability of Atmospheric Transparency and Precipitable Water in Estonia During the Last Decades*. PhD dissertation. Tartu University Press.
- Rosa, R. and Stanhill, G. 2014. Estimating long-wave radiation at the Earth's surface from measurements of specific humidity. *Int. J. Climatol.*, **34**, 1651–1656.
- Ruckstuhl, C., Philipona, R., Morland, J., and Ohmura, A. 2007. Observed relationship between surface specific humidity, integrated water vapor, and longwave downward radiation at different altitudes. *J. Geophys. Res.-Atmos.*, **112**(D3), D03302.
- Russak, V. and Kallis, A. 2003. *Eesti kiirguskliima teatmik [Handbook of Estonian Solar Radiation Climate]*. Eesti Vabariigi Keskkonnaministeerium, Tallinn (in Estonian).
- Stanhill, G. 2011. The role of water vapor and solar radiation in determining temperature changes and trends measured at Armagh, 1881–2000. *J. Geophys. Res.-Atmos.*, **116**, D03105.

Aluspinna ja atmosfääri pikalaineline kiirgus Eestis

Viivi Russak ja Ingrid Niklus

Juba mitmeid aastakümneid on maailma paljudes kohtades mõõdetud päikesekiirgust, oluliselt vähemates paikades ja lühemat aega aga pikalainelist kiirgust. Ometi on just viimane tähtis nii kiirgusbilansi kui ka kasvuhooneefekti kujunemisel. Pikalainelise kiirguse mõõtmine hoogustus pärast seda, kui 1992. aastal käivitatus ülemaailmse meteoroloogiaorganisatsiooni algatatud päikesekiirguse baasjaamade võrgu projekt (BSRN).

Eestis algasid päikesekiirguse pidevad mõõtmised 1950. aastal. Ligikaudu poole sajandi jooksul talletatud mõõtmisandmete põhjal on selle ajalisi ja territoriaalseid iseärasusi kirjeldatud "Eesti kiirguskliima teatmik" (Russak, Kallis 2003). Pikalainelise kiirguse andmearad on aga tunduvalt lühemad: aluspinnale jõudva atmosfääri pikalainelise kiirguse ehk vastukiirguse $L_1\downarrow$ mõõtmine algas Eesti Keskkonnaagentuuri Tartu-Tõravere meteojaamas 2003. aastal, aluspinna pikalainelise kiirguse $L_1\uparrow$ oma aga 2006. aasta juulis. Et infrapunase kiirguse muutlikkus aastast aastasse on päikesekiirgusega võrreldes suhteliselt väike, on võimalik juba praeguseks kogutud andmete põhjal kirjeldada selle Eestile iseloomulikke jooni.

Eestis langeb aasta jooksul aluspinnale päikesekiirgusest keskmiselt kolm korda rohkem atmosfääri pikalainelist kiirgust. See vahetõde muutub aasta jooksul suurtes piirides, olenedes eelkõige Päikese kõrgusest ja päeva pikkusest, aga ka pilvisusest. Kui suvel erinevad Päikese ja atmosfääri vastukiirguse summad vähe, siis talvekuudel on

päikesekiirguse osa praktiliselt tähtsusetu, moodustades vaid mõne protsendi kogu kiirgusest. Aluspinnalt lahkuvas kiirguses on aluspinna pikalainelise kiirguse suhteline osa veelgi suurem, ulatudes aastasummas keskmiselt 92%-ni. Päikesekiirgusega võrreldes on pikalainelise kiirguse aastane käik vähem ilmekas. Samuti on väiksem selle varieeruvus aastast aastasse. Nii $L_1\uparrow$ kui ka $L_1\downarrow$ tunnisummade sagedusjaotus on keskmiselt monomodaalne, küll aga muutub aasta jooksul selle kuju. Nii näiteks on nende jaotused veebruaris pilvitutest pakasepäevadest tingituna bimodaalsed.

Aluspinna pikalaineline kiirgus $L_1\uparrow$ oleneb peamiselt kiirgava pinna temperatuurist t ja vähesel määral selle kiirgusvõimest ε . Eestis aastail 2007–2012 esinenud temperatuuride piires (-27 kuni $+32$ °C) on kiirguse olenevus temperatuurist lineaarne:

$$L_1\uparrow = 0,017 t + 1,146, \quad R^2 = 0,98. \quad (1)$$

Mõõdetud ja lumepinna jaoks Stefani-Boltzmanni valemiga (kiirgusvõime $\varepsilon = 0,85$) arvutatud $L_1\uparrow$ tunnisummad olid heas kooskõlas ($R^2 = 0,96$), kuid mõõdetud väärtused olid süstemaatiliselt suuremad (keskmiselt 18%), mis võib olla tingitud ε valikust.

Atmosfääri vastukiirgus $L_1\downarrow$ kujuneb mitme teguri koosmõjul, millest kõige olulisem on veeaur. Eestis on $L_1\downarrow$ tunnisummade (MJ m^{-2}) olenevus aluspinnalähedasest veeauru rõhust e (hPa) ligikaudu kirjeldatav astmefunktsiooniga:

$$L_1\downarrow = 0,704 e^{0,23}, \quad R^2 = 0,73. \quad (2)$$

Sarnane seos on saadud ka mõnede autorite teistes geograafilistes kohtades tehtud mõõtmiste analüüsist. Erinevused on aga funktsiooni parameetrite väärtustes, mis on arvatavasti tingitud õhuniiskuse ja -temperatuuri vertikaalsete profiilide ning pilvisuse erinevustest.

Hindamiseks pilvede mõju $L_1\downarrow$ kujunemisele analüüsiti eraldi nende tundide andmeid, kui taevas oli pilvitu või üleni madalate pilvedega kaetud ($m = 10$). Mõlemal juhul osutus jällegi sobivaks lähendiks astmefunktsioon:

$$L_1\downarrow = 0,796 e^{0,20}, \quad R^2 = 0,93, \quad m = 10, \quad (3)$$

$$L_1\downarrow = 0,601 e^{0,25}, \quad R^2 = 0,91, \quad \text{pilvitu.} \quad (4)$$

Korrelatsioon atmosfääri pikalainelise kiirguse ja veeauru rõhu vahel oli tugevam talvekuudel. Soojal aastaajal väheneb aluspinnalähedase veeauru tähtsus vastukiirguse $L_1\downarrow$ kujunemisel, sest konvektiivne turbulents kannab niiskust atmosfääri kõrgematesse kihtidesse.

Eesti Keskkonnaagentuuri Tartu-Tõravere meteojaam on üks vähestest Põhja-Euroopas, kus mõõdetakse pikalainelist kiirgust. Kuna Läänemere piirkonnas on ilma peamiseks kujundajaks Atlandi ookeani kohalt ida suunas liikuvad tsüklonid, on siinsed atmosfääri vastukiirgust mõjutavad meteoroloogilised parameetrid (temperatuur, niiskus, pilvisus jm) üsna sarnased. Seepärast oletame, et pikalainelise kiirguse eelkirjeldatud omadused on ligikaudu iseloomulikud tervele sellele alale.